International Journal of Science and Research Archive
eISSN: 2582-8185
Cross Ref DOI: 10.30574/ijsra
Journal homepage: https://ijsra.net/

(RESEARCH ARTICLE)

Check for updates

POM-132@MOF-801 HYBRID FOR PRESSURE-DEPENDENT NOX CAPTURE: SYNTHESIS, STRUCTURAL CHARACTERIZATION AND STATIC-PRESSURE ADSORPTION PERFORMANCE

Sumayya Fayyaz [1, 2, *], Tehseen Ullah [1,2, 3], Farhana Fazal [1, 3], Muhammad Saad Azeem [2, 3], Muhammad Huzaifa [2, 3] and Iftikhar Ali [2, 3]

[1] School of Materials Science and Engineering, Anhui University of Science and Technology, Huainan, 232001, Anhui, China.
[2] School of Earth and Environmental Science, Anhui University of Science and Technology, Huainan, 232001, Anhui, China.
[3] International Islamic University Islamabad, Pakistan.
* Corresponding Author

ORCID Details
Sumayya Fayyaz: https://orcid.org/0009-0000-5849-2560

International Journal of Science and Research Archive, 2026, 20(03), 152–160

Publication history: Received on 27 July 2026; revised on 02 September 2026; accepted on 05 September 2026

Article DOI: https://doi.org/10.30574/ijsra.2026.20.3.1711

ABSTRACT

Nitrogen oxides (NOx) are important atmospheric pollutants generated predominantly by combustion and industrial processes and are associated with ozone formation, secondary particulate matter, acid deposition, and adverse environmental and health effects. The development of porous materials capable of capturing nitrogen oxides therefore remains an important research objective. Metal–organic frameworks (MOFs) provide structurally tunable porous environments, while polyoxometalates (POMs) offer oxygen-rich surfaces together with distinctive acid–base and redox properties. Their integration provides an attractive route toward multifunctional adsorption materials. In this study, a Mo132-containing MOF composite, denoted Mo132@MOF-801, was synthesized and investigated for static-pressure NOx uptake. MOF-801 was prepared from zirconium tetrachloride and fumaric acid using N, N-dimethylformamide/water and acid modulation, while boric acid was also employed during synthesis. The Mo132-containing POM was prepared from ammonium molybdate, ammonium acetate, and hydrazine sulfate under acidic aging conditions. The resulting POM/MOF hybrid was subsequently prepared by thermal treatment in ethanol. Fourier-transform infrared spectroscopy (FTIR), powder X-ray diffraction (PXRD), scanning electron microscopy (SEM), and energy-dispersive X-ray spectroscopy (EDS) were employed to characterize the materials. The composite exhibited a distinct FTIR fingerprint and retained crystalline features after hybridization. SEM revealed a heterogeneous, aggregated morphology, while EDS detected O, Cl, Zr, and Mo, with normalized mass fractions of 33.71, 13.45, 20.39, and 32.45%, respectively. Static-pressure NOx measurements at 273 K yielded reported uptake values of 10, 14, 19, 21 and 21 mmol g^{-1} at 0.5, 1.0, 1.5, 2.0 and 2.5 bar, respectively. The uptake increased by 110% between 0.5 and 2.0 bar and exhibited an apparent plateau between 2.0 and 2.5 bar. The results indicate that the Mo132@MOF-801 architecture can accommodate substantial NOx uptake under the reported static conditions. Nevertheless, because the adsorbent mass was varied systematically across the pressure measurements and the exact NOx composition, activation

procedure, replicate measurements, and uncertainty were not reported, the data should be interpreted as pressure-dependent static uptake rather than as a rigorously resolved equilibrium isotherm. The study establishes a promising POM/MOF design concept while identifying the experimental requirements necessary for quantitative validation and practical evaluation.

Keywords: MOF-801; Mo132; Polyoxometalate; POM/MOF Hybrid; Nox Adsorption; Nitrogen Oxides; Zirconium Fumarate; Gas Capture; Porous Materials

1 INTRODUCTION

Nitrogen oxides (NOx), principally nitric oxide (NO) and nitrogen dioxide (NO2), are among the most important gaseous pollutants associated with combustion, transportation and industrial activity. Beyond their direct environmental effects, NOx participates in atmospheric photochemistry and contributes to ozone formation, secondary aerosol formation, and acid deposition. Consequently, technologies capable of capturing, separating, or converting NOx remain important for environmental protection and emission control [1–3]. Adsorption is particularly attractive for gas purification because porous solids can capture target molecules through a combination of pore confinement and specific adsorbate–surface interactions. Conventional adsorbents such as activated carbon and zeolites have demonstrated utility, but their chemical environments are comparatively difficult to tune. Metal–organic frameworks (MOFs), in contrast, provide a versatile platform in which metal clusters, organic linkers, pore dimensions, surface functionality, and defect chemistry can be systematically modified [4,5]. The exceptional structural diversity and tunability of MOFs have consequently stimulated extensive research into gas storage, separation, sensing and environmental remediation. The adsorption of toxic gases by MOFs is strongly influenced by both pore architecture and surface chemistry. Reviews of toxic-gas adsorption have shown that functionalization, defect engineering and incorporation of chemically active sites can substantially alter adsorption performance [3,6]. In particular, adsorption of NOx requires consideration not only of available pore volume but also of interactions between the highly polarizable gas molecules and chemically active sites. Zirconium-based MOFs are attractive for such applications because Zr–O coordination networks generally exhibit high chemical and thermal stability. MOF-801 is a zirconium–fumarate framework containing small tetrahedral and octahedral pores, making it particularly interesting for adsorption of small molecules [7,8]. The reported pore dimensions and adsorption characteristics of MOF-801 have resulted in applications including water and hydrogen storage and other adsorption processes.

The chemical identity of MOF-801 is particularly relevant to the present study. Published work identifies MOF-801 as a Zr-fumarate framework, and fast synthesis routes have demonstrated that ZrCl4, fumaric acid, DMF, water, and carboxylic-acid modulators can produce crystalline MOF-801 [7,8]. The experimental thesis used ZrCl4, DMF, water, acid modulation, and boric acid in the preparation of the MOF material. Fumaric acid was also used experimentally as the organic linker but was inadvertently omitted from the written thesis procedure; the present manuscript corrects that omission. The exact quantity of fumaric acid is not reproduced because it is not available from the surviving experimental record and is not recalled by the authors. An additional strategy for modifying porous materials is the incorporation of polyoxometalates. POMs are discrete metal-oxide clusters characterized by oxygen-rich surfaces, high charge density, tunable acidity, and redox activity [9,10]. Their molecular properties make them attractive for catalysis, adsorption, sensing, and environmental applications. However, unsupported POMs can suffer from relatively low accessible surface area, aggregation and handling/recovery difficulties. Incorporation of POMs into MOFs offers a way of combining the functionality of POMs with the structural advantages of porous hosts. POM@MOF hybrids can provide confined POM environments, improved dispersion and modified host–guest interactions [11]. The POM component investigated in this work is referred to as Mo132. Mo132 belongs to the family of large Keplerate-type polyoxomolybdates and possesses a highly oxygenated molybdenum-oxide framework with a characteristic hollow molecular architecture. Published Mo132 studies demonstrate its synthesis from molybdate precursors under hydrazine/acetate/acetic-acid conditions similar to those employed in the present work [12]. The thesis employed ammonium molybdate hydrate, ammonium acetate, hydrazine sulfate, and 50% acetic acid, followed by four days of aging at 28 °C to obtain the brown POM-132 powder.

POM-containing materials are also relevant to NOx adsorption. Zhu et al. demonstrated that heteropolyacid-based materials can adsorb NOx and that support–POM interactions influence adsorption behavior [13]. Their study reported significant NOx uptake by supported heteropolyacid materials and used spectroscopic measurements to investigate NOx/POM interactions. Earlier infrared studies likewise demonstrated that nitrogen oxides can interact with heteropolyacid surfaces, highlighting the importance of chemically active POM environments in NOx capture [14]. These observations provide the scientific rationale for combining a porous zirconium framework with a Mo-containing POM. The present work therefore investigates a Mo132@MOF-801 hybrid prepared by combining the porous architecture of MOF-801 with the oxygen-rich chemistry of a Mo132-containing POM. The study focuses on synthesis, structural characterization, and static-pressure NOx uptake. The objectives were to: synthesize MOF-801; synthesize the Mo132-containing POM; prepare the Mo132@MOF-801 hybrid; characterize the parent materials and composite

using FTIR, PXRD, SEM, and EDS; investigate pressure-dependent NOx uptake at 273 K; and develop a structure–property interpretation of the observed adsorption behavior.

2 MATERIALS

Zirconium tetrachloride (ZrCl4), acetic acid, boric acid, N, N-dimethylformamide (DMF), methanol, and other synthesis reagents were obtained from commercial suppliers as reported in the thesis. The thesis identifies Sigma-Aldrich as the supplier for the principal MOF-related chemicals. The POM synthesis employed ammonium molybdate hydrate, ammonium acetate, hydrazine sulfate, and acetic acid. Ethanol was used during POM washing and composite preparation. All chemicals were used without further purification unless otherwise specified.

2.1 Synthesis of MOF-801

MOF-801 was synthesized using zirconium tetrachloride (ZrCl4) as the zirconium precursor and fumaric acid as the organic linker. Boric acid was also employed during the synthesis, while acetic acid was used as a modulating component. Briefly, 10 g of ZrCl4 was mixed with 10 mL of DMF under magnetic stirring for approximately 10 min. Subsequently, 10 mL of deionized water was added, and the mixture was stirred for approximately 30 min. Fumaric acid was then introduced as the organic linker together with boric acid, followed by approximately 1–2 mL of acetic acid. After homogenization, the reaction vessel was sealed and heated at 120 °C for 2 h. The resulting white precipitate was recovered by centrifugation, cooled to room temperature, washed three times with DMF and once with methanol, and finally dried at 60 °C. The resulting zirconium–fumarate framework was designated MOF-801. The original thesis omitted fumaric acid from the written experimental procedure; its use is restored here based on the experimental record provided by the authors. The quantities of fumaric acid and boric acid are not reported because their exact amounts could not be recovered and are therefore not estimated. The ZrCl4/DMF/water/modulator conditions are consistent with published fast MOF-801 synthesis strategies employing fumaric acid and carboxylic-acid modulators [7].

2.2 Synthesis of Mo132-type POM

The POM was prepared by dissolving 11.3 g of ammonium molybdate hydrate and 24.0 g of ammonium acetate in 400 mL of double-distilled water. Subsequently, 1.6 g of hydrazine sulfate was added dropwise under stirring. After approximately 10 min, the solution developed a blue-green color. Subsequently, 166 mL of 50% acetic acid was added, producing a green solution. The reaction mixture was aged at 28 °C for four days, after which a brown precipitate formed. The precipitate was recovered by centrifugation and washed thoroughly with water and ethanol to obtain the POM-132 powder. The synthesis chemistry is consistent with published preparation routes for Mo132-type Keplerate polyoxomolybdates [12]. Because the present dataset does not include single-crystal X-ray diffraction or a complete molecular-level structural analysis of the isolated POM, the designation Mo132-type POM is used where structural certainty is required.

2.3 Preparation of Mo132@MOF-801

Seven grams of POM-132 and 6 g of MOF-801 were combined under magnetic stirring in ethanol. After mixing, the vessel was sealed and heated at 120 °C for 3 h. After cooling to room temperature, the resulting greenish powder was separated by centrifugation. This represents the initial synthesis ratio and should not be interpreted as the actual POM loading of the final composite.

3 RESULTS AND DISCUSSION

3.1 FTIR characterization

The FTIR spectra of pristine MOF-801, POM-132, and the MOF-801@POM-132 composite are presented in Figure X. The spectrum of pristine MOF-801 exhibits the characteristic broad absorption in the ~3600–3200 cm^{-1} region, which can be associated with O–H stretching vibrations arising from adsorbed water and/or hydroxylated Zr clusters. The prominent bands in the ~1600–1550 and ~1450–1380 cm^{-1} regions are characteristic of the asymmetric and symmetric stretching vibrations of coordinated carboxylate groups, respectively, originating from the fumarate linker coordinated to the Zr_6 inorganic nodes. The presence of these coordinated COO^- vibrations, rather than a strong free-carboxylic-acid band near ~1720 cm^{-1}, is consistent with the formation of the Zr–fumarate framework characteristic of MOF-801 [15]. Furthermore, the absorption bands observed in the lower-wavenumber region, particularly around ~800–650 and ~550–450 cm^{-1}, can be attributed to vibrations associated with the Zr–O/Zr–O–C coordination environment and the Zr_6 oxo/hydroxo clusters of the MOF framework [16,17].

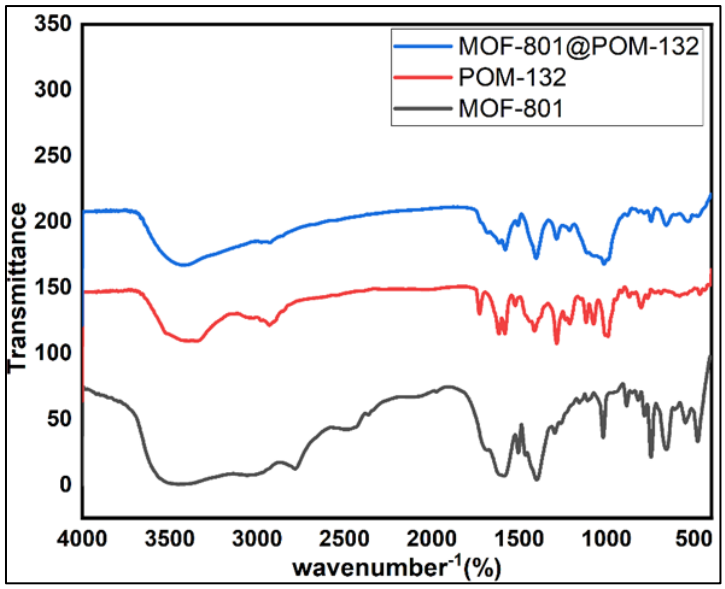

Figure 1: FTIR of MOF-801, POM-132 and POM-132@MOF-801

The POM-132 spectrum displays a substantially different fingerprint, particularly in the ~1700–500 cm^{-1} region, indicating its distinct molecular/inorganic structure. The multiple absorption features observed in the fingerprint region can therefore be considered characteristic vibrations of the POM-132 constituent. After formation of the MOF-801@POM-132 composite, the resulting spectrum retains the principal vibrational features of both MOF-801 and POM-132. Importantly, the characteristic bands of the composite exhibit changes in relative intensity and, in some regions, slight displacement or broadening compared with the pristine components. This spectral evolution suggests that POM-132 has been successfully incorporated or immobilized within/on the MOF-801 matrix and that interfacial interactions occur between the two components. Such changes may originate from electrostatic interactions, hydrogen bonding, coordination-related interactions, or confinement effects at the MOF–POM interface [18]. However, because no completely new, well-resolved absorption bands are evident from the present spectrum alone, the FTIR results should not be used to claim unequivocal formation of a new covalent bond between MOF-801 and POM-132. Rather, the preservation of the characteristic MOF-801 framework vibrations together with the appearance/retention of POM-132-related features supports the successful formation of the MOF-801@POM-132 hybrid while indicating that the fundamental chemical structure of the MOF-801 framework remains largely preserved.

3.2 PXRD characterization

To study the crystallization and phases of synthesized sample XRD characterization is used. The sample were characterized by using XRD (PSD MEGA PC 1) in International Islamic university Islamabad. The sample was placed in a diffractometer and characterized according to the working principle described in the above section. All measurements were taken between 2θ values of 10-90°.

The X-ray diffraction results, plot the intensity of MOF 801 and its composite of the signal for various diffraction angles at their respective theta positions. The XRD image of (A) MOF, and (B) MOF/POM Composite are shown in figure 4.2.1. The signal intensity for the angles of graph A, θ 38.35°, θ 44.79°, θ 44.79°, θ 78.36° which is allocated by MOF 801), B: θ 33.00°, θ 58.82°, θ 78.43 which is assigned by MOF 801 composite. The diffraction angles are comparable with previous literature [15].

The intensity of MOF/POM composite is gradually increase due to adding of ethanol. It is means that tensile stress is introduced and the capacity of MOF/POM Composite can be improved.

The X-ray diffraction results, plot the intensity of POM and its composite of the signal for various diffraction angles at their respective theta positions. The XRD image of (A) POM, and (B) MOF/POM Composite are shown in Fig 2. The signal intensity for the angles of graph A, θ 12.41°, θ 43.53°, θ 65.03°, θ 78.11° which is allocated by MOF 801), B: θ 33.09°, θ 58.86°, θ 78.11 which is assigned by MOF 801 composite.

The intensity of MOF/POM composite is gradually increased due to adding of ethanol. It means that tensile stress is introduced and the capacity of MOF/POM Composite can be improved. While one peak vanishes on of MOF/POM Composite due to the high growth of ethanol and moves to a higher peak. The diffraction angles are comparable with previous literature [15].

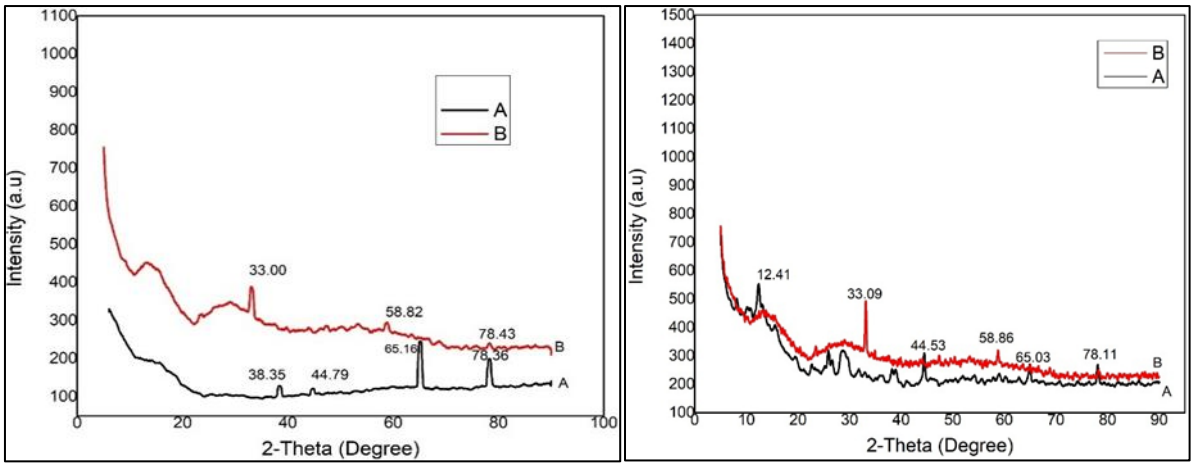

Figure 2: (a) XRD of MOF-801 and POM-132@MOF-801, (b) XRD of POM-132 and POM-132@ MOF-801.

The difference between the diffraction patterns of the parent materials and the composite indicates a modified crystalline response following hybridization. Such changes may arise from differences in crystallite size, phase abundance, preferred orientation, macrostrain, or particle packing. The original thesis attributed increased diffraction intensity to tensile stress introduced by ethanol. However, intensity changes alone are insufficient to establish tensile stress. A more rigorous interpretation is therefore that composite formation modifies the crystallinity and/or relative contribution of the constituent phases. Quantitative line-profile analysis would be required before assigning the observed changes specifically to strain. Published MOF-801 studies emphasize the importance of crystallinity, synthesis conditions, and modulator chemistry in controlling the properties of the zirconium–fumarate framework [7,8].

3.3 SEM morphology

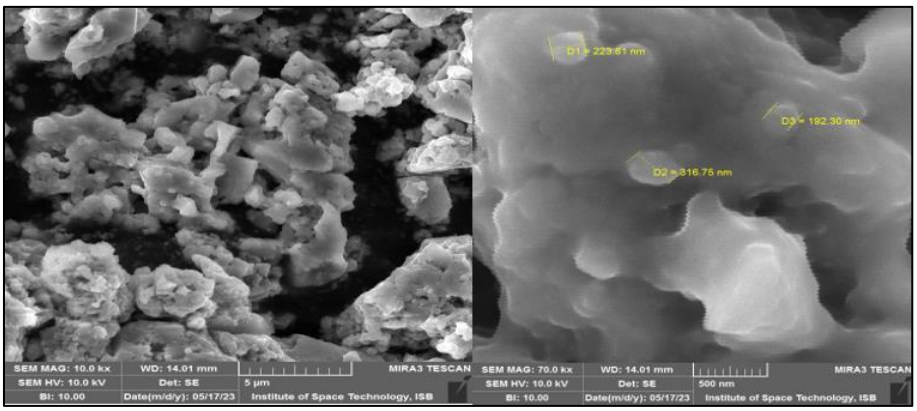

Figure 3: SEM of POM132@MOF-801

The scanning electron microscopy (SEM) images of the synthesized MOF-801@POM-132 composite reveal a heterogeneous and highly aggregated morphology with irregularly shaped particles and rough, non-uniform surfaces as shown in fig 3. At 10,000× magnification, the composite consists of interconnected aggregates with relatively large interparticle voids, indicating substantial particle agglomeration. This morphology differs from the relatively well-defined spherical morphology commonly reported for pristine MOF-801, for which uniform nanoparticles with an average particle size of approximately 150 nm have been reported [19]. More recent studies have also shown that the morphology of MOF-801 can vary considerably with synthesis conditions, with particle sizes in the tens to hundreds of nanometers being reported [20]. Therefore, the irregular morphology observed in the present MOF-801@POM-132 sample may be associated with modification of the MOF surface and particle–particle interactions following incorporation of POM-132. Similar aggregated structures with rough surfaces have been observed in POM@MOF composites, where the incorporation of polyoxometalate species resulted in massive structures consisting of aggregated nanoparticles with rough surface characteristics [21].

The higher-magnification SEM image (70,000×; 500 nm scale bar) provides clearer evidence of the surface heterogeneity of MOF-801@POM-132. The selected morphological features exhibit dimensions of approximately 192.30, 223.81, and 316.75 nm. These values should be regarded as representative dimensions of selected morphological domains rather than an average particle size because the particles are strongly interconnected and

individual crystallites cannot be clearly distinguished in the micrograph. The relatively rough and compact surface observed at higher magnification may result from the association of POM-132 with the external surface and/or within accessible regions of the MOF-801 structure during composite formation. Morphological modification following incorporation of POM species has also been reported for POM@MOF materials, although the extent of morphological change depends strongly on the MOF, POM identity, and preparation route [22,23]. Importantly, SEM morphology alone cannot conclusively demonstrate that POM-132 is encapsulated inside the pores of MOF-801. SEM should therefore be combined with energy-dispersive X-ray spectroscopy (EDS) elemental mapping, which can provide spatial information about the characteristic elements of the POM and MOF components and has been widely used to evaluate the distribution of POM species in MOF-based composites.

3.4 EDS elemental composition

EDS analysis of a selected region of the composite gave the following composition:

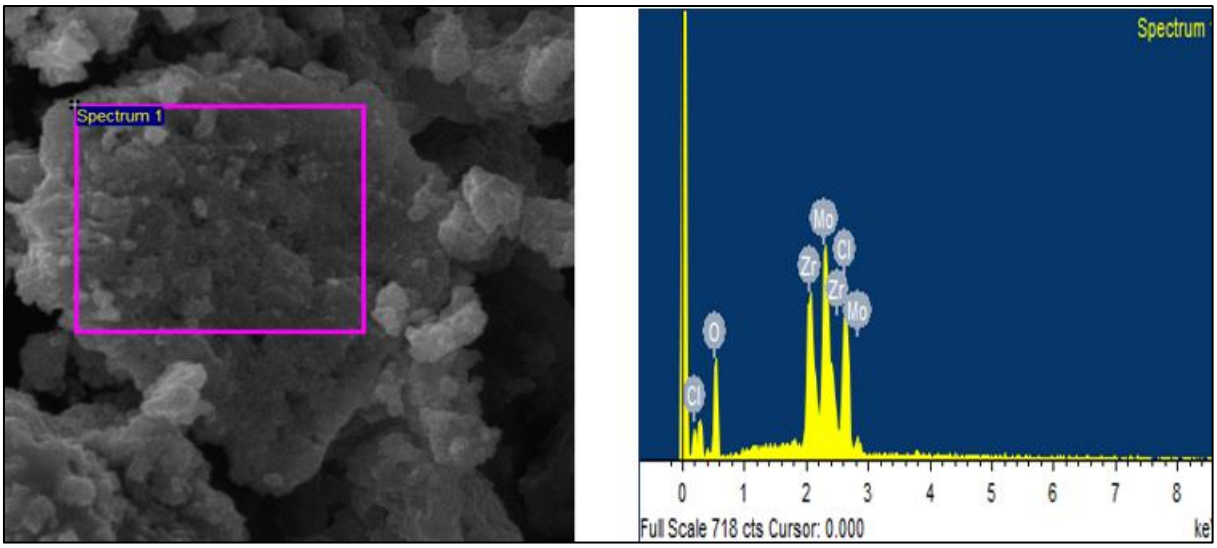

Figure 4: EDS analysis of a selected region

Table 1: EDS elemental composition of Mo132@MOF-801

Element	Weight (%)	Atomic (%)
O	33.71	69.12
Cl	13.45	12.45
Zr	20.39	7.33
Mo	32.45	11.10

The simultaneous detection of Zr and Mo provides direct compositional evidence that the analyzed region contains both the zirconium-containing MOF component and the molybdenum-containing POM component. The relatively high Mo signal is consistent with the presence of a substantial Mo-containing phase. The chlorine signal is also noteworthy. Because ZrCl4 was used as the zirconium precursor, residual chloride-containing species could potentially contribute to the detected chlorine. Alternatively, chlorine may arise from incomplete washing or localized precursor residues. EDS is inherently local and semi-quantitative; therefore, it should not be used to determine the bulk Mo loading of the composite. ICP-OES or ICP-MS would provide more reliable bulk compositional data.

3.5 Static-pressure NOx adsorption

The central functional result of the study is the reported NOx uptake at 273 K.

Table 2: Reported static-pressure NOx uptake of Mo132@MOF-801 at 273 K

Pressure (bar)	Reported adsorbent mass (mg)	NOx uptake (mmol g^{-1})
0.5	0.3	10
1.0	0.6	14
1.5	0.9	19
2.0	1.2	21
2.5	1.5	21

The values are reported in the thesis experimental record.

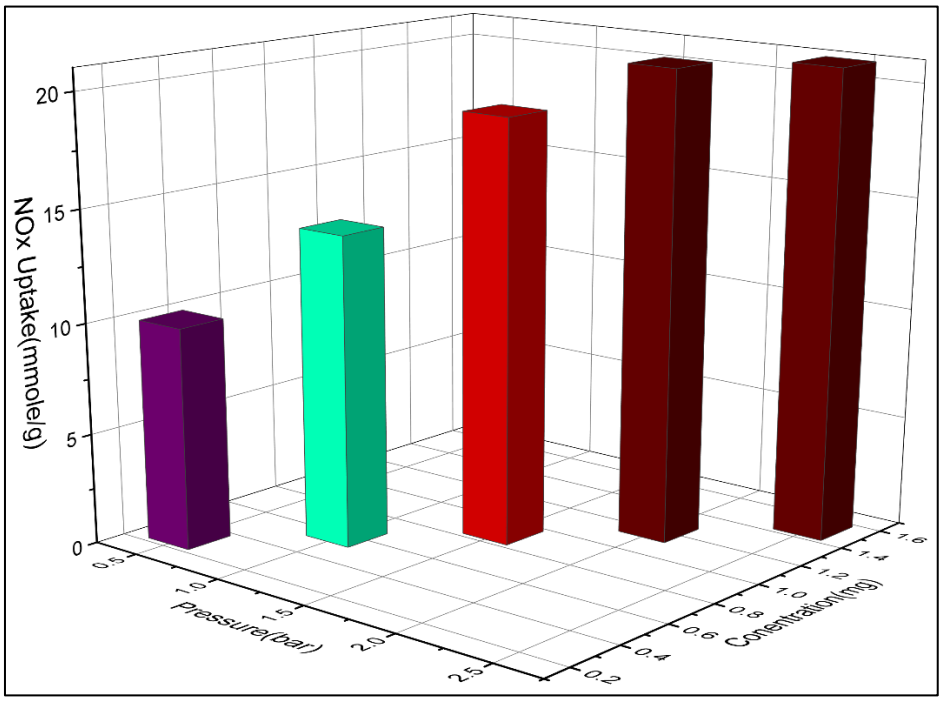

Figure 5: Reported static-pressure NOx uptake of POM-132@MOF-801 at 273 K.

The reported uptake increased from 10 mmol g^{-1} at 0.5 bar to 21 mmol g^{-1} at 2.0 bar, corresponding to an increase of: The reported uptake subsequently remained at 21 mmol g^{-1} at 2.5 bar. The pressure-dependent trend can therefore be summarized as follows: The apparent plateau above 2 bar is qualitatively consistent with progressive occupation of accessible adsorption sites. However, there is an important methodological consideration: the adsorbent mass changes from 0.3 to 1.5 mg as pressure increases. Consequently, pressure and adsorbent mass are not independent variables in the reported experiment. For this reason, the results should not be described as a conventional equilibrium adsorption isotherm. Instead, the scientifically accurate description is: "static-pressure-dependent NOx uptake measurements." This distinction is essential for a high-quality publication. A rigorous equilibrium isotherm should use a fixed, activated adsorbent mass and measure equilibrium uptake at progressively increasing pressure under otherwise identical conditions.

4 CONCLUSION

A Mo132@MOF-801 hybrid was synthesized through integration of a zirconium–fumarate MOF with a Mo-containing polyoxometalate. The corrected experimental description identifies fumaric acid as the organic linker used in MOF-801 synthesis, while boric acid and acetic acid were also employed during the preparation. The omission of fumaric acid from the original thesis experimental description was inadvertent. The Mo132-type POM was prepared using ammonium molybdate, ammonium acetate, hydrazine sulfate, and acetic acid, followed by controlled aging. The resulting POM was combined with MOF-801 in ethanol at 120 °C to produce the greenish hybrid powder. FTIR measurements demonstrated distinct vibrational fingerprints for the parent materials and composite, while PXRD confirmed that crystalline features were retained following hybridization. SEM revealed heterogeneous aggregated morphology, and EDS detected O, Cl, Zr, and Mo within the analyzed composite region. The reported static-pressure

NOx uptake at 273 K increased from 10 mmol g^{-1} at 0.5 bar to 21 mmol g^{-1} at 2.0 and 2.5 bar. This represents a reported 110% increase relative to the 0.5-bar measurement. The pressure dependence is consistent with progressive occupation of accessible adsorption sites; however, the measurements cannot presently be interpreted as a rigorous equilibrium adsorption isotherm because the adsorbent mass varied systematically with pressure. The exact NOx composition, activation procedure, uncertainty, and reproducibility must also be established. The principal scientific contribution of this work is therefore the demonstration of a Mo132@MOF-801 hybrid architecture for NOx capture, combining a zirconium–fumarate porous host with an oxygen-rich molybdenum-containing POM. The study provides a foundation for further development of POM/MOF adsorbents, but future work should focus on quantitative pore characterization, Mo loading, rigorous equilibrium adsorption measurements, regeneration, humidity tolerance, selectivity, and direct mechanistic characterization.

STATEMENTS ON COMPLIANCE WITH ETHICAL STANDARDS

Disclosure of conflict of interest

The authors declare that they have no known competing financial or personal interests that could have appeared to influence the work reported in this paper.

Consent to publish

All authors have read and approved the final version of the manuscript and consent to its publication.

REFERENCES

[1] Lin, J.; Ho, W.; Qin, X.; et al. Metal–Organic Frameworks for NOx Adsorption and Their Applications in Separation, Sensing, Catalysis, and Biology. Small **2022**, 18, 2105484. DOI: 10.1002/smll.202105484.

[2] Dağlar, H.; Altintas, C.; Erucar, I.; et al. Metal-organic framework-based materials for the abatement of air pollution and decontamination of wastewater. Chemosphere **2022**, 303, 135082. DOI: 10.1016/j.chemosphere.2022.135082.

[3] Binaeian, E.; El-Sayed, E. S. M.; Khanpour Matikolaei, M.; Yuan, D. Experimental strategies for enhancing toxic gas uptake of metal–organic frameworks. Coordination Chemistry Reviews **2021**, 430, 213738. DOI: 10.1016/j.ccr.2020.213738.

[4] Furukawa, H.; Cordova, K. E.; O'Keeffe, M.; Yaghi, O. M. The Chemistry and Applications of Metal-Organic Frameworks. Science **2013**, 341, 1230444. DOI: 10.1126/science.1230444.

[5] Rowsell, J. L. C.; Yaghi, O. M. Effects of Functionalization, Catenation, and Variation of the Metal Oxide and Organic Linking Units on the Low-Pressure Hydrogen Adsorption Properties of Metal–Organic Frameworks. J. Am. Chem. Soc. **2006**, 128, 1304–1315. DOI: 10.1021/ja056639q.

[6] Khan, N. A.; Hasan, Z.; Jhung, S. H. Adsorptive removal of hazardous materials using metal-organic frameworks (MOFs): A review. J. Hazard. Mater. **2013**, 244–245, 444–456.

[7] Kim, H.; Rao, S. R.; Kapustin, E. A.; et al. Adsorption-based atmospheric water harvesting device for arid climates. Nature Communications **2018**, 9, 1191. DOI: 10.1038/s41467-018-03162-7.

[8] Butova, V. V.; Pankin, I. A.; Burachevskaya, O. A.; Vetlitsyna-Novikova, K. S.; Soldatov, A. V. New fast synthesis of MOF-801 for water and hydrogen storage: Modulator effect and recycling options. Inorganica Chimica Acta **2021**, 514, 120025. DOI: 10.1016/j.ica.2020.120025.

[9] Song, Y.-F.; Tsunashima, R. Recent advances on polyoxometalate-based molecular and composite materials. Chem. Soc. Rev. **2012**, 41, 7384–7402. DOI: 10.1039/C2CS35143A.

[10] Omwoma, S.; Gore, C. T.; Ji, Y.; Hu, C.; Song, Y.-F. Environmentally benign polyoxometalate materials. Coordination Chemistry Reviews **2015**, 286, 17–29.

[11] Butova, V. V., Pankin, I. A., Burachevskaya, O. A., Vetlitsyna-Novikova, K. S., & Soldatov, A. V. (2021). New fast synthesis of MOF-801 for water and hydrogen storage: Modulator effect and recycling options. *Inorganica Chimica Acta*, *514*, 120025.

[12] Taghiyar, H.; Yadollahi, B.; Abbasi Kajani, A. Controlled drug delivery and cell adhesion for bone tissue regeneration by Keplerate polyoxometalate (Mo132)/metronidazole/PMMA scaffolds. Scientific Reports **2022**, 12, 14443. DOI: 10.1038/s41598-022-18622-w.

[13] Zhu, H.; Yu, M.; Ma, T.; Wang, R.; Korchak, V.; Korchak, V. N.; Matulis, V. E. Adsorption and Decomposition of NOx on Heteropolyacids: An Evaluation of the Adsorption Performance. Aerosol and Air Quality Research **2021**, 21, 210251. DOI: 10.4209/aaqr.210251.

[14] Herring, A. M.; McCormick, R. L. In Situ Infrared Study of the Absorption of Nitric Oxide by 12-Tungstophosphoric Acid. J. Phys. Chem. B **1998**, 102, 3175–3184. DOI: 10.1021/jp9727660.

[15] *Bordiga, S.; et al. Power of Infrared and Raman Spectroscopies to Characterize Metal–Organic Frameworks and Investigate Their Interaction with Guest Molecules.* ***Chemical Reviews*** *2022, 122, 6145–6277.*

[16] *Al-Mamun, M. R.; et al. Fumarate Based Metal–Organic Framework: An Effective Catalyst for the Transesterification of Used Vegetable Oil.* ***Crystals*** *2022, 12, 151.*

[17] *Ghosh, A.; et al. Detoxification of Chemical Warfare Agents by a Zr-Based MOF with High Recycling Ability at Physiological pH.* ***ChemNanoMat*** *2024.*

[18] *Biswas, S.; et al. MOF-801 as a Nanoporous Water-Based Carrier System for In Situ Encapsulation and Sustained Release of 5-FU for Effective Cancer Therapy.* ***Inorganic Chemistry*** *2022.*

[19] Ke, F., Peng, C., Zhang, T., Zhang, M., Zhou, C., Cai, H., Zhu, J., & Wan, X. (2018). Fumarate-based metal-organic frameworks as a new platform for highly selective removal of fluoride from brick tea. *Scientific Reports, 8*, 939. https://doi.org/10.1038/s41598-018-19277-2.

[20] Li, B., Wu, Z., Xu, X., Lv, Y., Guo, Y., Liang, S., Wang, Z., He, L., & Song, Y.-F. (2024). GSH/pH dual-activated POM@MOF for tumor cell-specific synergistic photothermal and chemodynamic therapy. *Inorganic Chemistry Frontiers, 11*, 4439–4448. https://doi.org/10.1039/D4QI01079E.

[21] Dong, Z., Zeng, D., Li, Z., Chen, J., Wang, Y., Cao, X., Yang, G., Zhang, Z., Liu, Y., & Yang, F. (2024). Polyoxometalate-encapsulated metal–organic frameworks for photocatalytic uranium isolation. *Chemical Science, 15*, 19126–19135. https://doi.org/10.1039/D4SC05349D.

[22] Kruse, S. M., et al. (2023). Polyoxometalate–soft matter composite materials: Design strategies, applications, and future directions. *Advanced Functional Materials*. https://doi.org/10.1002/adfm.202208428.

[23] Li, et al. (2025). Atmospheric water sorption kinetics in powder and monolithic metal–organic frameworks. *Advanced Materials Interfaces*. https://doi.org/10.1002/admi.202400628.